

# Quantitative Analysis of Microstructural Evolution at Cu/Al Solid-Liquid Bonding Interface

Wang Chan<sup>1,2</sup>, Liang Shuhua<sup>1,2</sup>, Zou Juntao<sup>1,2</sup>, Jiang Yihui<sup>1,2</sup>, Yang Qing<sup>1,2</sup>

<sup>1</sup>Xi'an University of Technology, Xi'an 710048, China; <sup>2</sup>Shaanxi Province Key Laboratory of Electrical Materials and Infiltration Technology, Xi'an 710048, China

**Abstract:** The Cu/Al diffusion couples were prepared by a solid-liquid bonding method. Interfacial microstructure and phase composition were investigated by scanning electron microscope (SEM), energy dispersive spectrometry (EDS) and X-ray differential (XRD). Moreover, the microstructural evolution of Cu/Al interface was quantitatively analyzed on the basis of diffusion theory and phase diagram. The results reveal that the interface consists of I (AlCu+Al<sub>2</sub>Cu), hypereutectic microstructure II [Al<sub>2</sub>Cu+( $\alpha$ -Al+Al<sub>2</sub>Cu)] and hypoeutectic microstructure III [ $\alpha$ -Al+( $\alpha$ -Al+Al<sub>2</sub>Cu)] from Cu side to Al side accordingly. Further, there are various morphologies of Al<sub>2</sub>Cu phase formed with the decreasing of Cu concentration. Additionally, the thickness of three diffusion zones is basically identical with the theoretical prediction.

**Key words:** Cu/Al alloy; solid-liquid interface; diffusion equation; microstructural evolution

Cu-Al bimetal has been widely applied in many industrial fields because of its excellent properties such as high electrical conductivity, good corrosion resistance and high strength-to-weight ratio<sup>[1-3]</sup>. Unfortunately, as a brittle phase, Al<sub>2</sub>Cu phase is easily generated at the Cu/Al interface, which seriously affects the property of composites<sup>[4,5]</sup>. Consequently, much attention has been paid to the growth behavior of Al<sub>2</sub>Cu phase. The variation of microstructure caused by preparation parameters and the effect of magnetic field as well as solidification rate on Al<sub>2</sub>Cu phase, were reported in Refs. [6-9]. For instance, Li et al. investigated the micro-structure of Al-Al<sub>2</sub>Cu eutectic alloy in high axial magnetic field, and found that the field can modify the preferred orientation of Al<sub>2</sub>Cu phase<sup>[6]</sup>. The effect of directional solidification rate on microstructures of Al-40%Cu hypereutectic alloy was investigated by Gao et al.<sup>[7]</sup>, which revealed the morphology change in phase growth from faceted primary Al<sub>2</sub>Cu phase to non-faceted phase with reducing-growth rate. Furthermore, first-principles study and thermodynamic assessment of Al-Cu systems are available in Refs. [10,11].

However, the deep understanding of the microstructural evolution, especially the growth behavior of Al<sub>2</sub>Cu phase depends on the accurate understanding of diffusion phenomenon at interface. Considerable investigations pointed out that diffusion may induce significant changes in composition and microstructure in the vicinity of the interface of bimetals, and it is closely related to the phase formation as well, thus eventually exerting influence on the properties of the composite<sup>[12-15]</sup>. Consequently, the diffusion phenomenon occurring at Cu/Al interface has attracted much interest. Many efforts have been done to understand the diffusion behavior by evaluating the diffusion coefficient of elements. Various methods, such as X-ray radiography, microtome sectioning and capillary reservoir technique were developed<sup>[16-18]</sup>. However, one of bimetals should be liquid or solid, which is affected by many inevitable factors. Nevertheless, much research has been done on the microstructural evolution of Cu/Al interface, and the hypo- or hyper-eutectic alloys are merely discussed separately (i.e. Al-2wt%Cu<sup>[19]</sup>, Al-10wt%Cu<sup>[20]</sup>, Al-35wt%Cu<sup>[7]</sup> and Al-40wt%Cu<sup>[21]</sup>) in a particular case. Therefore, for Cu/Al

Received date: April 25, 2017

Foundation item: National Natural Science Foundation of China (51371139, 51174161); the Science and Technique Innovation Program of Shaanxi Province (2012KTQ01-14); the Pivot Innovation Team of Shaanxi Electric Materials and the Infiltration Technique (2012KCT-25)

Corresponding author: Liang Shuhua, Ph. D., Professor, School of Materials Science and Engineering, Xi'an University of Technology, Xi'an 710048, P. R. China, Tel: 0086-29-82312181, E-mail: liangsh@xaut.edu.cn

Copyright © 2018, Northwest Institute for Nonferrous Metal Research. Published by Elsevier BV. All rights reserved.

integral structure rather than a certain composition, not much attention has been shed on the microstructural evolution based on the quantitative analysis.

In this study, we investigated the Cu/Al diffusion couple prepared by the solid-liquid bonding, since it is a promising technique with sound metallurgical bonding and high efficiency<sup>[22,23]</sup>. Moreover, the quantitative analysis of microstructural evolution at interface was discussed based on the diffusion theory and the Cu-Al phase diagram. These results will provide theoretical foundation and guide for a better understanding of the formation mechanism at Cu/Al liquid/solid interface on the one hand and contribute to understanding the design and control of the microstructure in Cu-Al bimetals on the other hand. In addition, it is the purpose of this study to provide this microstructural evolution of the Cu/Al interface, which will serve as a key binary edge system of the Cu-W-Al ternary system in our later research as well.

## 1 Experiment

Pure Al ingot (99.99 wt%) and Cu rod (99.99 wt%) were cut into Al column (20 mm in diameter, 30 mm in height) and Cu column (20 mm in diameter, 8mm in height), respectively. To remove oxide film, the specimens were etched firstly in 10 wt% NaOH and then in 10 wt% HCl solution. Moreover, through ultrasonical treatment, the surface was thoroughly cleaned. Copper and aluminum were placed into a metal crucible with an inner diameter of 20 mm. Thereafter, the bonding tests were carried out in argon atmosphere on a SK-G10123K type tube furnace. The bonding process was conducted at 690 °C with different holding time (20, 40 and 60

min), followed by water quenching.

In order to investigate the microstructural evolution in the diffusion zone, the cross sections of the interface were prepared using conventional metallographic techniques. The sample was etched by reagent (0.5 mL HF and 99.5 mL distilled water). The microstructure of the diffusion zone was observed by a JEOL JSM6700 field emission scanning electron microscope (SEM). The compositions at interface were analyzed by energy dispersive spectrometry (EDS), and the phase was finally identified by X-ray diffraction (XRD).

## 2 Results and Discussion

### 2.1 Interfacial microstructures

The interfacial morphology of the specimen bonded for 60 min is shown in Fig.1a. Cu substrate is on the left, and the right is Al substrate. The interface diffusion layer grows along the perpendicular direction of initial interface and the thickness is approximately equal to several thousand microns. In order to facilitate the quantitative discussion in greater detail, the interface was divided into three zones on the basis of various growth modes and structures of the intermetallic phase, which are zone I, II and III from Cu side to Al side accordingly, and the morphologies are shown in Fig.1b~1g.

The composition of the zones was analyzed using EDS technique to obtain the quality percentage of points, as shown in Table 1. Moreover, the phase diagram and XRD analysis were applied to further identify the phases of zones, as shown in Fig.2 and Fig.3.

According to Cu content in Table 1, it can be deduced that

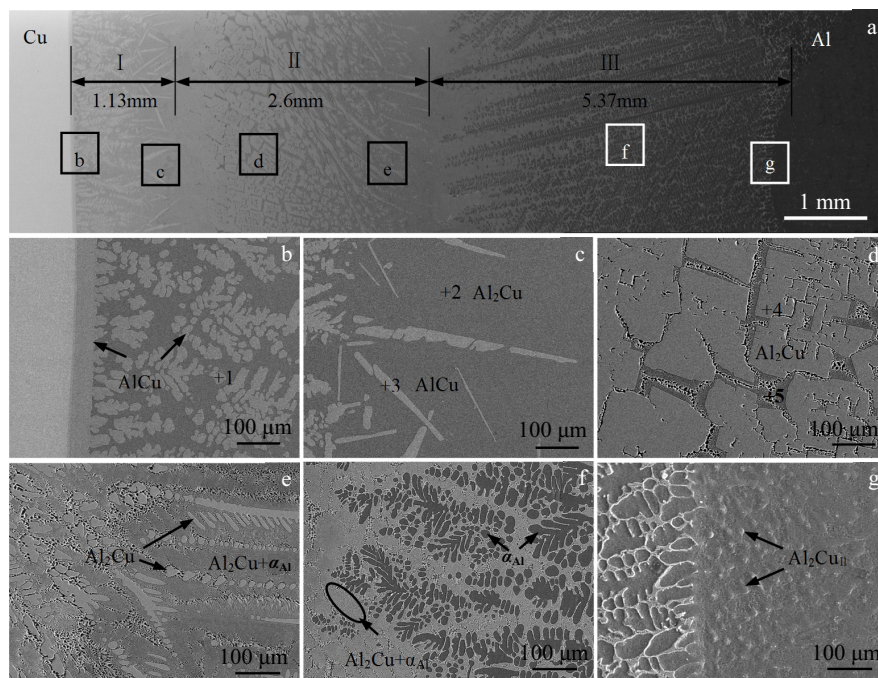


Fig.1 Microstructures (a) of Cu/Al interface at 690 °C treated for 60 min; (b~g) are different locations b~g microstructures of three zones from Cu side to Al side accordingly in Fig.1a

**Table 1 EDS results of points marked in Fig.1b~1d**

Point	1	2	3	4	5
Al content/wt%	28.66	46.32	28.53	47.42	52.94
Cu content/wt%	71.34	53.68	71.47	52.58	47.06
Phase	AlCu	Al <sub>2</sub> Cu	AlCu	Al <sub>2</sub> Cu	Al+Al <sub>2</sub> Cu

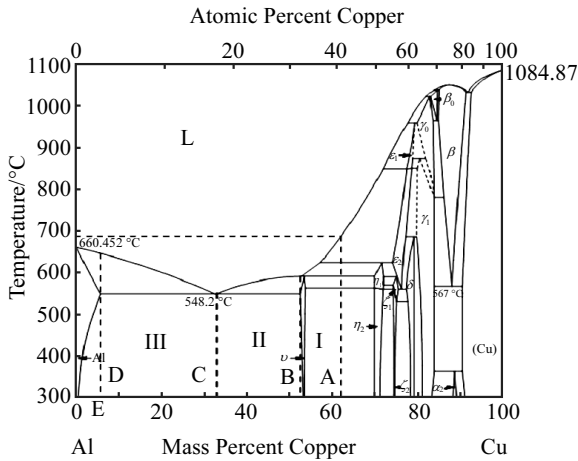


Fig.2 Al-Cu binary alloy phase diagram; I, II and III represents three zones of Cu/Al interface and the points marked by A~E are the critical value of several zones<sup>[24]</sup>

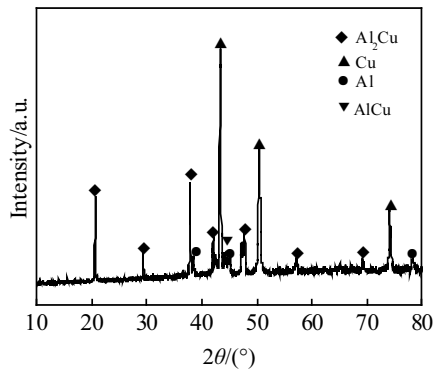


Fig.3 XRD patterns of Cu/Al interface at 690°C treated for 60 min

point 1 and 3 are AlCu phase, while point 2 and 4 are Al<sub>2</sub>Cu phase. Point 5 should be composed of Al and Al<sub>2</sub>Cu phase according to the Cu-Al phase diagram<sup>[24]</sup>, and the result of XRD analysis indicates this as well, as shown in Fig.3.

XRD result indicates that the interface intermetallic phases are mainly composed of Al<sub>2</sub>Cu and AlCu phases, which is consistent with EDS analysis. It can also be noticed that the number of strip and acicular structure is less than that of the plane and square structure from the interfacial morphology (Fig.1a~1e). Consequently, three zones of the interface are identified to be I (AlCu+Al<sub>2</sub>Cu), II [Al<sub>2</sub>Cu+(α-Al+Al<sub>2</sub>Cu)] hypereutectic microstructure and III [α-Al+(α-Al+Al<sub>2</sub>Cu)] hypoeutectic microstructure. Accordingly, the mean thickness of several zones is 1.13, 2.6 and 5.37 mm, respectively, as illustrated in Fig.1a.

In combination with the Cu-Al phase diagram, the concentration of Cu in the several microstructures as mentioned is 70 wt%~53.3 wt%, 53.3 wt%~33.2 wt% and 33.2 wt%~5.6 wt%, respectively. It is found that the Cu concentration gradually decreases with the increase of the diffusion distance from zone I to zone III. In addition, it will the liquid flow of the integrated material caused by disturbance outside will not occur during the melting and solidification. Consequently, it can be deduced that the distribution of Cu atom is completely dominated by the diffusion, and thus the formation of Cu/Al bimetal interface can be explained by the diffusion theory.

## 2.2 Concentration variation of Cu based on the diffusion theory

During the formation of the Cu/Al solid-liquid interface, there exists two kinds of diffusion conditions, i.e. Cu diffuses to liquid Al, while Al also diffuses to solid Cu. The diffusion coefficients of them were calculated by Arrhenius equation:

$$D = D_0 \exp\left(-\frac{Q}{RT}\right) \quad (1)$$

where  $D_0$  is the pre-exponential factor and  $Q$  is the activation energy.  $R$  and  $T$  are the gas constant and the absolute temperature, respectively. The value of  $T$  was set at 963 K in the experiment. The diffusion of Cu in liquid Al: the values of  $D_0^{(1)}$  and  $Q^{(1)}$  are determined to be  $1.1 \times 10^{-7} \text{ m}^2/\text{s}$  and  $2.38 \times 10^4 \text{ J/mol}$ <sup>[25]</sup>, respectively. The diffusion of Al in fcc Cu: the values of  $D_0^{(2)}$  and  $Q^{(2)}$  are determined to be  $1.3 \times 10^{-5} \text{ m}^2/\text{s}$  and  $1.85 \times 10^5 \text{ J/mol}$ , respectively<sup>[26]</sup>. The diffusion coefficient can be calculated from Eq. (1) and the values are  $D^{(1)} = 5.63 \times 10^{-9} \text{ m}^2/\text{s}$  and  $D^{(2)} = 1.21 \times 10^{-15} \text{ m}^2/\text{s}$ . Obviously, the diffusion coefficient of Cu in liquid Al is six orders of magnitude larger than that of Al in fcc Cu. Therefore, the contribution of Al atoms diffusing into solid Cu to interfacial formation can be negligible.

For the Cu-Al binary diffusion systems, the variation of Cu concentration, which varies with the distance and time in front of interface, is a dimensional unsteady diffusion process that is in line with Fick's second law, and it can be expressed as:

$$\frac{\partial c}{\partial t} = D \frac{\partial^2 c}{\partial x^2} \quad (2)$$

The end of aluminium far from copper side is not affected by the diffusion in formation of the interface, where the concentration of Cu is equal to zero. Therefore, this diffusion situation can be seen as a mode of semi-infinite diffusion. The schematic diagram of the diffusion is shown in Fig.4. Initial and boundary conditions are as follows:

$$t=0, x \geq 0, c=c_1=0; t>0, x=0, c=c_0; x=\infty, c=c_1=0$$

Consequently, the solution meets partial differential Eq. (2) as well as the initial and boundary condition is error function solution, and the detailed mathematical derivation is stated in Ref. [27]. Therefore the distribution of Cu concentration in front of interface can be obtained as:

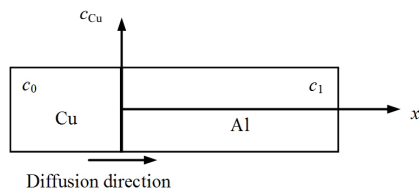


Fig.4 Schematic illustration of Cu atom diffuse

$$c(x,t) = c_0 [1 - \operatorname{erf}(\frac{x}{2\sqrt{Dt}})] \quad (3)$$

Where  $x$  is the distance from Cu/Al solid-liquid interface,  $c_0$  is the Cu concentration in initial interface,  $t$  is the holding time which was set at  $t=3600$  s, and  $D$  is the diffusion coefficient. The value of  $D$  is determined to be  $5.63 \times 10^{-9}$  m<sup>2</sup>/s.  $c_0$  is obtained from the Cu-Al phase diagram (as shown in Fig.2 point A). Accordingly, the variation curves of Cu concentration with the diffusion distance can be obtained and given in Fig.5. It indicates that the concentration of Cu appears to obey a monotonic decreasing relationship while the distance from initial interface is increasing. The critical values of Cu concentration can be obtained based on the Cu-Al phase diagram, and they are  $c^I=53.3$  wt%,  $c^{II}=33.2$  wt% and  $c^{III}=5.6$  wt%. The diffusion distance of several zones is illustrated in Fig.5.

When the samples were bonded for 60 min at 690 °C, the concentration variation of Cu is consistent with the experimental results, which can be noticed by combining Fig.1a with Fig.5. Furthermore, the thickness of each zone is basically identical with the theoretical prediction. Therefore, the Eq.(3) can be used to explain the formation of Cu/Al solid-liquid interface.

### 2.3 Microstructural evolution

The quantitative analysis of microstructural evolution depends on the Cu-Al phase diagram as well as the results of concentration variation of Cu based on the diffusion theory, and the discussion is as follows.

According to the Cu-Al phase diagram, the concentration of

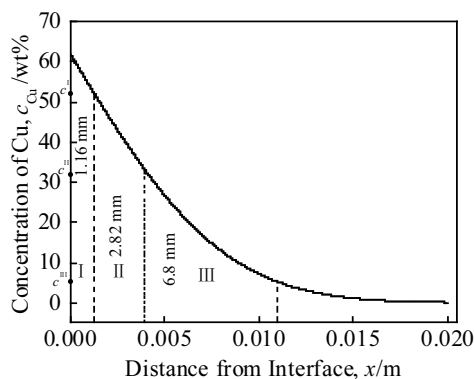


Fig.5 Mass fraction of Cu in the solid-liquid interface as a function of diffusion distance with holding time for 60 min

Cu at the initial interface is 62 wt% (point A), where the AlCu and Al<sub>2</sub>Cu phases coexist. According to the law of the lever, the concentration of AlCu and Al<sub>2</sub>Cu is 52.1 wt% and 47.9 wt%, respectively. The concentration of Cu is gradually decreased as distance from the interface increases. The AlCu phase becomes less, whereas the Al<sub>2</sub>Cu phase becomes more. Since the concentration of Cu varies continuously, the number of Al<sub>2</sub>Cu phase is more than that of AlCu phase. The coexistence region of intermetallic will not disappear until the concentration of Cu decreases to 53.3 wt%. Finally, the zone I forms which is composed of Al<sub>2</sub>Cu+AlCu mixed microstructure, and the thickness is 1.13 mm (Fig.1a). It is obvious that the structure of AlCu is strip near the Cu substrate (Fig.1b), while the acicular AlCu phase gradually appears far away from the Cu substrate (Fig.1c). In comparison, the plane structure of Al<sub>2</sub>Cu phase forms. According to the distribution of Cu concentration, 61.65 wt% is the critical value above which the amount of AlCu phase is less than that of Al<sub>2</sub>Cu phase; furthermore, it is close to the initial concentration of interface. Hence, the number of AlCu phase is less than that of Al<sub>2</sub>Cu phase with the decreasing of Cu concentration. In addition, the layer of AlCu phase with thickness of 44.74 μm is formed close to the Cu substrate, as shown in Fig. 1b. This can be ascribed to the equal binding energy of Cu and Al (Cu: 336 kJ/mol, Al: 327 kJ/mol)<sup>[28]</sup>; accordingly, the activation energy of them is nearly equal. The number of the activated atoms is 1:1 at the early stage in rapid solidification; therefore, the intermetallic layer of AlCu phase forms immediately, and it moves forward layer by layer. Due to the continuous diffusion of Cu atom, Al atom begins to be rich in front of interface with the growth of the AlCu phase near the initial interface. Al<sub>2</sub>Cu phase begins to develop when the number ratio of Al to Cu atoms tends to be 2:1. The concentration of Cu in front of interface declines with the increasing of diffusion distance. However, AlCu phase with short strip and acicular structure is generated in certain zone of striped layer<sup>[21]</sup>.

Along with the continuous diffusion of Cu element, when the concentration varies from 53.3 wt% to 33.2 wt%, it is evident that the number of eutectic phase becomes more while that of AlCu phase becomes less. When the concentration of Cu reaches the eutectic composition (33.2 wt%), the zone II with thickness of 2.6 mm occurs which is mainly [Al<sub>2</sub>Cu+(Al<sub>2</sub>Cu+α-Al)] hypereutectic microstructure, as can be seen in Fig.1a. The primary Al<sub>2</sub>Cu forms with square-shaped and approximate spherical structure, as shown in Fig.1d~1e. The eutectic structure (α-Al+Al<sub>2</sub>Cu) is developed by the crystallization of low melting point melt that is approximate to the eutectic composition at the final stage of solidification. The eutectic reaction of metals does not occur at the entire interface at the same time, but occurs in few points and then gradually expands, and the lamella-like with eutectic morphology finally degenerates between the primary Al<sub>2</sub>Cu, as illustrated in Fig.1d. It is indicated that the structure of Al<sub>2</sub>Cu varies with the various

concentration of interface. Different growth patterns of  $\text{Al}_2\text{Cu}$  phase, including L-shaped, E-shaped, and rectangular morphologies were observed by Gao<sup>[29]</sup>. Hamar et al.<sup>[30]</sup> thought that this depends on the composition of the alloy. As a result, the growth rate of crystal plane is different, which is the reason that the  $\text{Al}_2\text{Cu}$  phase presents various morphologies. Thus it can be deduced that the phase morphology is mainly dominated by the transformation of the crystal orientation caused by the various composition. According to the crystallography,  $\text{Al}_2\text{Cu}$  phase has crystallographic anisotropy, and the growth pattern is in line with the small plane, which was interpreted by the oriented attachment mechanism; as a result, the  $\text{Al}_2\text{Cu}$  phase presents diverse growth patterns and specific growth direction in different conditions<sup>[20]</sup>.

When the concentration of Cu varies from 33.2 wt% to 5.6 wt%, for instance, it decreases from 20 wt% to 10 wt%. According to the law of the lever, the eutectic structure decreases from 52.2 wt% to 15.9 wt%, while the  $\text{Al}_2\text{Cu}$  phase increases from 47.8 wt% to 84.1 wt%. It is evident that the number of eutectic phase becomes less while that of primary Al becomes more. Obviously, it is consistent with the results shown in Fig.1f~1g. The eutectic structure does not disappear until the concentration of Cu reduces a certain value (5.6 wt%), and the single-phase area of  $\alpha$ -Al gradually appears. As mentioned above,  $\text{Al}_2\text{Cu}$  phase has various growth patterns; however, the primary  $\alpha$ -Al of hypoeutectic structure always presents developed dendrites. There exists a rough interface between  $\alpha$ -Al and liquid, which is considered to be an isotropous non-crystallography interface, and thus the growth rate is the same. Consequently,  $\alpha$ -Al with similar oval-shape appears, in fact, it is dendrite. The eutectic structure transforms from dense lamellar structure to discontinuous reticular structure. The growth of dendrite arm is stopped due to the interaction of solute<sup>[31]</sup>.

It is evident that the eutectic structure always exists in the solidification microstructure when the concentration of Cu is 53.3 wt%~5.6 wt%. Take the eutectic point as the critical value, the zone is divided into two parts on the basis of different primary phase. When the concentration is less than 5.6 wt%, the secondary  $\text{Al}_2\text{Cu}$  phase will precipitate from grain interior and boundary of  $\alpha$ -Al crystal, as illustrated in Fig.1g ( $\text{Al}_2\text{Cu}_{\text{II}}$ ).

When the concentration of Cu varies from the point of B to E (Fig.2), the interface is mainly composed of  $\text{Al}_2\text{Cu}$  and  $\alpha$ -Al phase. However, the number and distribution of phase vary with the change of composition, resulting in the extraordinarily different microstructures of various zones. Consequently, the concentration variation caused by Cu diffusion, eventually facilitates the evolution of interfacial microstructure. Based on the stated above, the microstructural evolution process is schematically shown in Fig.6.

## 2.4 Interfacial thickness with different holding time

To verify the universality of diffusion theory at Cu/Al

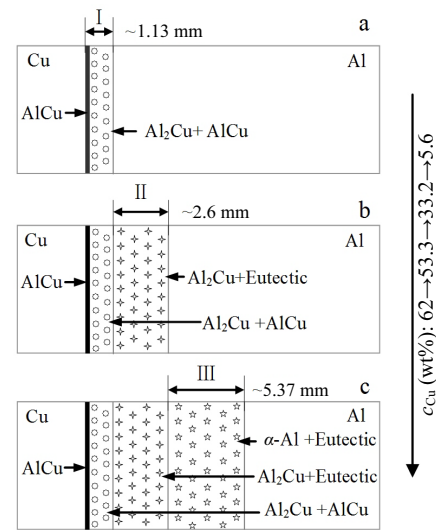


Fig.6 Schematic illustration of microstructural evolution with the decrease of Cu concentration in front of interface

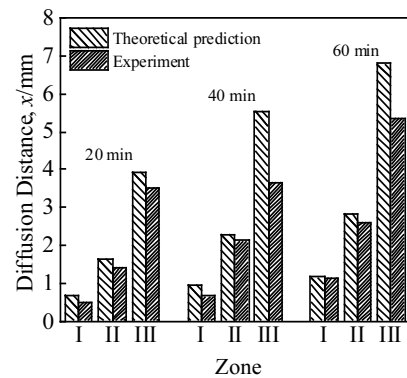


Fig.7 Diffusion distance of theoretical prediction and experiment at different holding time (20, 40 and 60 min)

interface, the samples held for 20 and 40 min was investigated as well. The thickness of several zones is gained by theoretical calculation and experimental measurement, as illustrated in Fig.7. It is obvious that the theoretical prediction is in good accordance with the experimental result at different holding time.

## 3 Conclusions

1) With the decreasing of Cu concentration in front of interface, three zones of the Cu/Al interface are identified to be I [ $\text{AlCu}+\text{Al}_2\text{Cu}$ ], II [ $\text{Al}_2\text{Cu}+(\text{Al}_2\text{Cu}+\alpha\text{-Al})$ ] hypereutectic microstructure and III [ $\alpha\text{-Al}+(\text{Al}_2\text{Cu}+\alpha\text{-Al})$ ] hypoeutectic microstructure, from Cu side to Al side accordingly.

2) The Cu concentration in front of Cu/Al interface decreases with increasing the distance from the initial interface. In addition, the thickness of several diffusion zones are 1.16, 2.82 and 6.8 mm, which is consistent with the experimental values.

3) Distinct holding time is similar in tendency when compared to the results between the theoretical prediction and experimental values. It further verifies the rationality of quantitative analysis of microstructural evolution at the Cu/Al interface.

## References

- Lee K S, Lee S E, Sung H K et al. *Materials Science and Engineering A*[J], 2013, 583: 177
- Saeid T, Abdollah-zadeh A, Sazgari B et al. *Journal of Alloys and Compounds*[J], 2010, 490: 652
- Ji F, Xue S B, Dai W. *Rare Metal Materials and Engineering*[J], 2013, 42(12): 2453
- He P, Liu D. *Materials Science and Engineering A*[J], 2006, 437(2): 430
- Zhang J, Huang Y N, Mao C et al. *Solid State Communications* [J], 2012, 152: 2100
- Li X, Ren Z M, Fautrelle Y et al. *Materials Letters*[J], 2010, 64: 2597
- Gao K, Song S J, Li S M et al. *Journal of Alloys and Compounds* [J], 2016, 660: 73
- Lee T H, Lee Y J, Park K J et al. *Journal of Materials Processing Technology*[J], 2013, 213(3): 487
- Guo Y J, Liu G W, Jin H Y et al. *Rare Metal Materials and Engineering*[J], 2012, 41(2): 281 (in Chinese)
- Gu J L, Bai J, Zhu Y et al. *Computational Materials Science*[J], 2016, 111: 328
- Liang S M, Schmid-Fetzer. *CALPHAD: Computer Coupling Phase Diagrams Thermochemistry*[J], 2015, 51: 252
- Guo Y J, Liu G W, Jin H Y et al. *Journal of Materials Science*[J], 2010, 46(8): 2467
- Su Y J, Liu X H, Huang H Y et al. *Metallurgical and Materials Transactions A*[J], 2011, 42: 4088
- Li J F, Agyakwa P A, Johnson C M. *Journal of Alloys and Compounds*[J], 2012, 545: 70
- Qi X S, Xue X Y, Tang B et al. *Rare Metal Materials and Engineering*[J], 2015, 44(7): 1575
- Zhang B, Griesche A, Meyer A. *Physical Review Letters*[J], 2010, 104(3): 035 902
- Murphy J B. *Acta Materialia*[J], 1961, 9(6): 563
- Wang T M, Cao F, Zhou P et al. *Journal of Alloys and Compounds*[J], 2014, 616: 550
- Wang F, Ma D X, Zhang J et al. *International Journal of Materials Research*[J], 2014, 105(2): 168
- Zhang Q, Liu S J, Yu S H. *Journal of Materials Chemistry*[J], 2009, 19: 191
- Palanisamy P, Howe J M. *Acta Materialia*[J], 2013, 61: 4339
- Sun J B, Song X Y, Wang T M et al. *Materials Letters*[J], 2012, 67(1): 21
- Marukovich E I, Branovitsky A M, Na Y S et al. *Materials and Design*[J], 2006, 27(10): 1016
- Brandes E A, Brook G B. *Smithells Metal Reference Book*[M]. USA: Butterworth-Heinemann, 1992
- Du Y, Chang Y A, Huang B Y et al. *Materials Science and Engineering A*[J], 2003, 363(1-2): 140
- Gerhard N, Cornelis T. *Pergamon Materials Series*[J], 2008, 14(14): 37
- Xu H Z. *Fundamentals of Materials Science*[M], Beijing: Beijing University of Technology Press, 2001, 143 (in Chinese)
- Hentzell H T G, Tu K N. *Journal of Alloys and Compounds*[J], 1983, 54(12): 6929
- Gao K, Li S M, Lei X et al. *Journal of Crystal Growth*[J], 2014, 394: 89
- Hamar R, Lemaignan C. *Journal of Crystal Growth*[J], 1981, 53(3): 586
- Bogno A, Nguyen-Thia H, Reinharta G et al. *Acta Materialia*[J], 2013, 61(4): 1303

## Cu/Al 固液连接界面组织演化的定量分析

王 婵<sup>1,2</sup>, 梁淑华<sup>1,2</sup>, 邹军涛<sup>1,2</sup>, 姜伊辉<sup>1,2</sup>, 杨 卿<sup>1,2</sup>

(1. 西安理工大学, 陕西 西安 710048)

(2. 陕西省电工材料与熔(浸)渗技术重点实验室, 陕西 西安 710048)

**摘 要:** 采用固-液法快冷成型制备了 Cu/Al 整体材料。利用 SEM, EDS, XRD 等分析了 Cu/Al 界面的微观结构和相组成, 基于扩散方程并结合相图定量分析了 Cu/Al 界面组织演化过程。结果表明: 从 Cu 侧至 Al 侧, 界面依次形成了区域 I (AlCu+Al<sub>2</sub>Cu)混合组织, 过共晶组织 [Al<sub>2</sub>Cu+(Al<sub>2</sub>Cu+ $\alpha$ -Al)] 的区域 II 和亚共晶组织 [ $\alpha$ -Al+(Al<sub>2</sub>Cu+ $\alpha$ -Al)] 的区域 III; 随着界面 Cu 浓度的变化, Al<sub>2</sub>Cu 相具有不同形貌; 且各个区域厚度同理论值基本一致。

**关键词:** Cu/Al; 固液界面; 扩散方程; 组织演化

作者简介: 王 婵, 女, 1989 年生, 博士生, 西安理工大学材料科学与工程学院, 陕西 西安 710048, 电话: 029-82312181, E-mail: wangcchan@126.com